Proceedings of the 28th IEEE
EMBS Annual International Conference
New York City, USA, Aug 30-Sept 3, 2006

3D Breast Microwave Imaging Based on Wavefront Reconstruction

Daniel Flores-Tapia, Gabriel Thomas, Ali Ashtari, Stephen Pistorius

Abstract-**Currently, breast cancer is the leading cause of cancer death in women between the ages of 15 and 54, and the second cause of cancer death in women 55 to 74. In recent years, Breast Microwave Imagery (BMI) has shown its potential as a promising breast cancer detection technique. This imaging technology is based on the electrical characteristic differences that exist between normal and malignant breast tissues at the microwave frequency range. A novel reconstruction approach for the formation of 3D BMI models is proposed in this paper. This technique uses the phase differences introduced during the collection of target responses in order to determine the correct spatial location of the different scatterers that constitute the final image. The proposed method yielded promising results when applied to simulated data.**

I. Introduction and Motivation

According to the World Health Organization, more than 1.2 million people were diagnosed with breast cancer the last year worldwide. The American Cancer Society estimated that in 2005, approximately 211,240 women in the United States were diagnosed invasive breast cancer [1]. Although mortality rates from breast cancer are currently at their lowest since the 1950s as a result of earlier detection through organized mammography screening programs and improved therapies following surgery, mammogram techniques still present limitations as a result of the low contrast between cancer and normal tissue observed in X-ray imagery. As mentioned in [2], mammogram images are difficult to interpret yielding as a consequence a high false negative rate (4%-34%) and a high false positive rate (70%). Alternative imaging modalities such as Magnetic Resonance Imaging (MRI) and ultrasound have shown promising results for breast cancer detection. However, MRI is too expensive and ultrasound does not have good spatial resolution to be considered for mass screening. In recent years, microwave approaches have been proposed for breast cancer detection.

Daniel Flores-Tapia, Gabriel Thomas and Ali Ashtari are with the Electrical and Computer Engineering Department, University of Manitoba, Winnipeg, Manitoba, R3T 5V6 Canada (phone: (204) 474-6893, fax: (204) 261-4639, e-mail: dflores@ee.umanitoba.ca, thomas@ee.umanitoba.ca), ashtari@ee.umanitoba.ca).

Stephen Pistorius is with the Department of Physics and Astronomy, University of Manitoba, Winnipeg, Manitoba, R3T 2N2; and CancerCare Manitoba, Winnipeg, Manitoba, R3E 0V9 Canada, (e-mail: stephen.pistorius@cancercare.mb.ca).

As shown by Surowiec et al [3] and further modeling done by Hagness et al [4], the dielectric properties of cancer and normal tissue exhibit a 5:1 contrast at the microwave frequency range. During the last years, some microwave approaches, such as microwave tomography and Ultra Wide Band (UWB) Radar [4,5], have been proposed.

Preliminary results obtained from both real and simulated data show the capability of this imaging modality to produce high contrast images. As discussed in [4], UWB Radar data is collected by illuminating the affected area with an UWB pulse. The irradiation is performed along a predefined trajectory following the breast contour. Tumor responses present different travel times due to the different position of the targets in the antenna radiation pattern at each scan location, resulting in the formation of nonlinear signatures. This phenomenon complicates the determination of the location and dimensions of each target present in the scanned area [4].

In order to visualize the targets reflections properly, the collected data must be focused [6]. For this purpose, both time and frequency domain techniques have been proposed [4,7]. Although most of the proposed methods generate 2D images, some steps have been taken to generate 3D BMI models [8]. UWB antennas generally present spherical radiation patterns which can make possible the collection of scatter responses that are off the scan plane. This property is highly desirable in a clinical environment due to the fact that no breast compression is needed in order to generate a 3D model.

This paper proposes the use of a novel wavefront reconstruction technique to focus and form breast microwave 3D models. This technique is an extension of the approach proposed by the authors in [7]. Contrary to time-shift techniques, wavefront reconstruction techniques focus the data by performing a series of operations in the frequency domain. Techniques based on the same theoretical basis have been used in [9] to focus 3D Synthetic Aperture Radar yielding high quality models.

This paper is organized as follows. The signal model is described in section 2. In section 3 the 3D wavefront reconstruction method is explained. The results of the artifact compensation and image formation using simulated data are shown and discussed in section 4. Finally, concluding remarks can be found in section 5.

II. SIGNAL MODEL

A cylindrical scan trajectory is the one considered in this paper. In this approach, the patient lies in a prone position and the antenna array is positioned in a concentrical array in the x-y plane around the circular shape adopted by the breast [6]. Let consider a circular array formed by N

antennas uniformly distributed in a circle of radius R. In this case, every element is facing towards the center of the array. T point scatterers are assumed to be located inside the area delimited by the array. For the following discussion, the center of the antenna array will be considered to be at the origin of the coordinate system. Also, a polar coordinate system will be used in order to simplify the calculations. Then, the location of the p scatter will be (r_p , ϕ_p, z_p) where $r = \sqrt{x_p^{\,2} + y_p^{\,2}}$ and $\phi = \tan^{-1}\left(y_p / x_p\right)$. In this case the distance between the n^{th} antenna and the p scatter is $D' = \sqrt{R^2 + r_p^{\,2} + (z_p - z_a)^2 - 2 \cdot R \cdot r_p \cos(\phi_p - \theta_n)}$, where ($R$, θ_n, z_a) are the cylindrical coordinates of the n^{th} antenna. A diagram of this model can be seen in figure 1.

A signal $f(t)$ is irradiated from each array element and the received signal by the n^{th} antenna can be expressed as:

$$s(t,\theta_n,z_a) = \sum_{j=1}^{T} \sigma_j f\left(t - \frac{2\sqrt{R^2 + r_j^{\,2} + (z_j - z_a)^2 - 2 \cdot R \cdot r_j \cos(\phi_j - \theta_n)}}{v}\right). \quad (1)$$

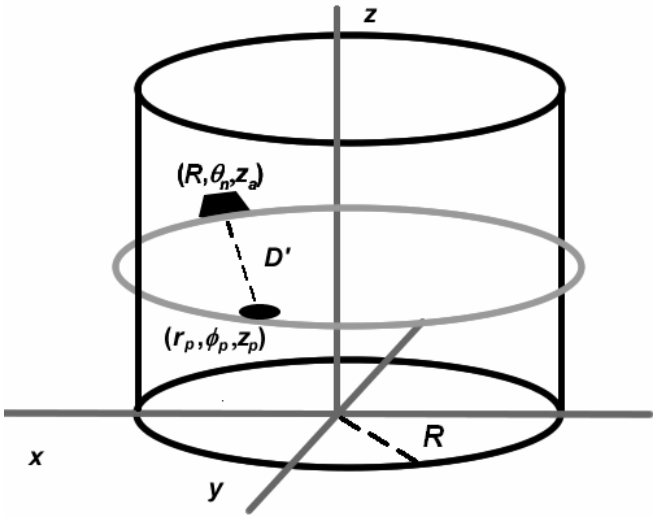

Figure 1. Geometry of the cylindrical array

Let consider now the response from the p scatter:

$$s_p(t,\theta_n,z_a) = \sigma_p \cdot f\left(t - \frac{2\sqrt{R^2 + r_p^{\,2} + (z_p - z_a)^{2^2} - 2 \cdot R \cdot r_p \cos(\phi_p - \theta_n)}}{v}\right). \quad (2)$$

The frequency representation of the previous signal can be obtained by calculating its Fourier transform which yields the following expression:

$$s_p(\omega,\theta_n) = \sigma_p F(\omega) e^{-2k\sqrt{R^2 + r_p^{\,2} + (z_p - z_a)^2 - 2 \cdot R \cdot r_p \cos(\phi_p - \theta_n)}} \quad (3)$$

where $k = \frac{\omega}{v}$ is often called the wavenumber.

III. WAVEFRONT RECONSTRUCTION

As mentioned in [3, 6], tumor reflections present nonlinear signatures due to the different signal travel times along the different scan locations. Therefore, in order to correctly asses the target dimensions and locations, the data must be focused. As illustrated in [10], the phase delay from each reflection can be used to accurately determine its spatial location. This is done by transferring the spectrum of the collected data from its original spatial temporal frequency space to a spatial frequency space related to the size of the scan area.

In order to perform this process, the Fourier transform of the collected data is calculated along the scan trajectory, yielding the following expression.

$$s_p(\omega,\varepsilon,k_z) = \int_0^{2\pi} \int_{z_i}^{z_f} \sigma_p F(\omega) \cdot e^{-j\left(2k\sqrt{R^2 + r_j^{\,2} + (z_j - z)^2 - 2 \cdot R \cdot r_p \cos(\phi_p - \theta_n)} + \varepsilon\theta + k_z z\right)} dz d\theta \quad (5)$$

where z_i and z_f are the initial and final scan locations in the z axis, and ε and k_z denote the spatial frequencies in the angular and z axis directions.

It can be noticed that equation 5 starts to oscillate rapidly around zero when k becomes large, as it would be on a UWB system, making difficult to evaluate the integral [11]. This fact is further explained in Appendix 1. However, it is possible to evaluate the frequency response of equation 5 by determining its asymptotic behavior [11]. For this purpose, the stationary phase method is used [11]. This method uses the behavior of the rate of change of the frequency, also known as Instantaneous Frequency (IF), of the angle function to determine the asymptotic behavior of the desired function. In general, the IF of a function $g(h(t))$ is given by $\frac{dh(t)}{dt}$. The behavior of the IF near the stationary points of the phase is analyzed in order to determine the asymptotic behavior of the desired function. For equation 5, the IF in the z direction is

$$\frac{(z_j - z^*)}{\sqrt{R^2 + r_j^{\,2} + (z_j - z^*)^2 - 2 \cdot R \cdot r_p \cos(\phi_p - \theta_n)}} - = \frac{k_z}{2k}, \quad (6)$$

where z^* is the stationary point location along the z direction. Notice how the left side of equation 6 resembles a sine relationship. Taking advantage of this fact to obtain the value of z^*, equation 6 can be rewritten as:

$$\sin\left(\tan^{-1}\left(\frac{(z_j - z^*)}{\sqrt{R^2 + r_j^{\,2} - 2 \cdot R \cdot r_p \cos(\phi_p - \theta_n)}}\right)\right) = \frac{k_z}{2k}, \quad (7)$$

yielding

$$z^* = z_j - \frac{k_z}{\sqrt{4k^2 - k_z^2}} \sqrt{R^2 + r_j^{\,2} - 2 \cdot R \cdot r_p \cos(\phi_p - \theta_n)}. \quad (8)$$

As mentioned in [11], the asymptotic behavior of an integral of the form: $M(k) = \int_a^b f(t) e^{jk\mu(t)} dt$, is given by the function $2 f(t_0) e^{jk\mu(t_0)}$, where t_0 is the stationary point of the phase function $\mu(t)$.

Using the stationary point value z^*, the asymptotic behavior of (5) in the z direction becomes:

$$s_p(\omega,\varepsilon,k_z)=2\int_0^{2\pi}\sigma_p F(\omega)\cdot e^{-j\left(\sqrt{4k^2-k_z^2}\sqrt{R^2+r_j^2-2Rr_p\cos(\phi_p-\theta_n)}+\varepsilon\theta+k_z z_j\right)}d\theta \quad (9)$$

where ε and k_z are the frequency counterparts of θ and z respectively. Next, the asymptotic behavior in the θ direction must be obtained. In this case, the IF of the PM component in the θ direction is:

$$\frac{d(-\sqrt{4k^2-k_z^2}\sqrt{R^2+r_p^2-2Rr_p\cos(\phi_p-\theta_n)}-\varepsilon\theta)}{d\theta}= -\frac{\sqrt{4k^2-k_z^2}\left(Rr_p\sin(\phi_p-\theta_n)\right)}{\sqrt{R^2+r_p^2-2Rr_p\cos(\phi_p-\theta_n)}}-\varepsilon \quad . \quad (10)$$

The stationary point θ^* is achieved when (10) reaches zero. Therefore:

$$\left[-\frac{\sqrt{4k^2-k_z^2}\left(Rr_p\sin(\phi_p-\theta_n)\right)}{\sqrt{R^2+r_p^2-2Rr_p\cos(\phi_p-\theta_n)}}-\varepsilon\right]_{\theta^*}=0 \quad (11)$$

From (11) the following relationship can be obtained:

$$\frac{\sin(\phi_p-\theta^*)}{\sqrt{Z^2+r_p^2-2Zr_p\cos(\phi_p-\theta^*)}}=\frac{\varepsilon}{2kZr_p}. \quad (12)$$

Obtaining the value of θ^* directly from (12) can be a tedious process. Nevertheless, notice how the left side of (12) resembles a sine law relationship. As it can be seen in [7], a triangle between the considered scatter, the antenna and the center of the scan pattern is formed. Therefore, from basic trigonometry it can be shown that $\theta^*=\phi_p+\alpha^*+\beta^*-\pi$, where α^* and β^* are the complimentary angles of θ^*. Given that the sine law applies for all the angles in the triangle, the values of α^* and β^* are: $\alpha^*=-\sin^{-1}\left(\frac{\varepsilon}{2kZ}\right)$ and $\beta^*=-\sin^{-1}\left(\frac{\varepsilon}{2kr_p}\right)$.

Substituting the value of θ^* in the phase modulated term in (9) yields:

$$s_p(\omega,\varepsilon,k_z)=4\sigma_p F(\omega)\cdot\exp\left[-i\left(\sqrt{\left(4k^2-k_z^2\right)r_p^2-\varepsilon^2}+\sqrt{\left(4k^2-k_z^2\right)R^2-\varepsilon^2}+ \sin^{-1}\left(\frac{\varepsilon}{\sqrt{4k^2-k_z^2}R}\right)+\sin^{-1}\left(\frac{\varepsilon}{\sqrt{4k^2-k_z^2}r_p}\right)+\pi+\varepsilon\phi_p+k_z z_j\right)\right] \quad (13)$$

where again ε is the frequency counterpart of θ.

As it can be seen, the π term in the phase of (13) produces a 180^o shift on the location of the target signatures. Due to the fact that the collected data is a function of the signal travel time from the antenna to the scatters, the data must be shifted in order to align it properly with the spatial origin of the data acquisition setup. This shift is related to the term $\sqrt{\left(4k^2-k_z^2\right)R^2-\varepsilon^2}$ present in equation (13). Also, as mentioned in [7], the term $\sin^{-1}\left(\frac{\varepsilon}{\sqrt{4k^2-k_z^2}R}\right)$ causes an additional spreading on the target signatures. In order to perform compensation, the 3D Fourier transform of the collected samples is obtained and multiplied by the kernel $e^{i\left(\sqrt{\left(4k^2-k_z^2\right)R^2-\varepsilon^2}+\pi+\sin^{-1}\left(\frac{\varepsilon}{\sqrt{4k^2-k_z^2}R}\right)\right)}$.

In order to transfer the compensated data ,$F(k,k_z,\varepsilon)$, from the (k,k_z,ε) frequency space to the (k_x,k_y,k_z) spatial frequency space for proper visualization, a remapping process must be performed. First, the frequency vector $k_{ur}=\sqrt{4k^2-k_z^2}$ is defined. Due to the fact that both k and k_z are evenly sampled, the values of k_{ur} will yield an unevenly spaced vector, unfit to be processed using FFT based techniques. In order to correct this issue, an evenly spaced vector $k_r=m\Delta k_r$ where $\Delta k_r=\pi/R$ and m is the length of the k vector, is generated. Then, the values of $F(\varepsilon,k_r,k_z)$ are interpolated from $F(\varepsilon,k_{ur}, k_z)$.

Next, the inverse FFT of the focused data is computed on the ε direction, resulting in a representation of the data in the (θ, k_r, k_z) domain. From this point, the following vectors are generated:

$$k_{ux}=k_r\cos(\theta) \text{ and } k_{uy}=k_r\sin(\theta). \quad (14)$$

As in the previous case, the k_{ux} and k_{uy} vectors are also unevenly spaced. In order to obtain an evenly sampled spectrum, the vectors $k_x=m\Delta k_x$ and $k_y=m\Delta k_y$ are defined, where $\Delta k_x=2\pi/X_0$, $\Delta k_y=2\pi/Y_0$ and X_0, Y_0 are the lengths of the data acquisition setup in the x and y directions respectively. Similarly to the previous case, $F(k_x, k_y, k_z)$ is obtained by interpolating the data in $F(k_{ux}, k_{uy}, k_z)$ into the evenly spaced frequency locations. Finally in order to visualize the data in the spatial domain, a 3D inverse FFT is applied to $F(k_x, k_y, k_z)$.

IV. RESULTS

In order to asses the capabilities of the proposed method, a set of simulated data was produced using a radar simulator developed by the authors. This data was generated using a simulated pattern of 72 scan locations with a radius of .4m in the x-y plane. The circular pattern scans were performed at 11 equidistant locations along a 10 cm aperture in the z-axis direction.

The dielectric permittivity values of the simulated breast and cancer tissues were 9 and 50 respectively. A Stepped Frequency Continuous Wave (SFCW) was used as the irradiated signal. The SCFW had a bandwidth of 11 GHz with a center frequency of 6.5 GHz. The proposed method was implemented in a Pentium 4 PC with 1 GB RAM using a Matlab development environment. The tumors were assumed to be point scatterers in all the experiments. An initial simulation was performed for two tumors positioned at (2,0.5) cm and (0,2.5) cm. A coronal view of the focused data at z=5cms and z=0cm can be seen in figure 2 a) and b) respectively. In order to visualize the benefits of the proposed technique in terms of focusing quality, the

proposed method was compared with the outcome of performing the 2D reconstruction method proposed in [7] in each scan plane. The results in the coronal view at z=5cm and z=0cm can be seen in figure 3 a) and b) respectively. The sagital view at y=0 for the 3D focused data and the 2D focused data can be seen in figure 4 a) and b) respectively. Notice how the 3D focusing process results in the formation of a more compact signature in the z-direction.

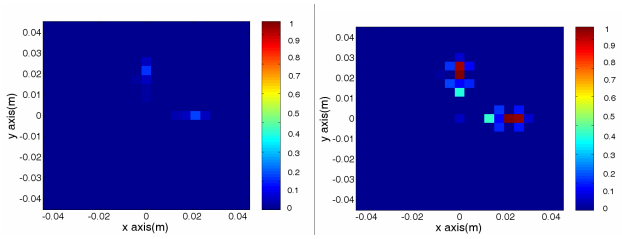

Figure 2. 3D focused data coronal view at: a) z=0 cm, b) z=5cm.

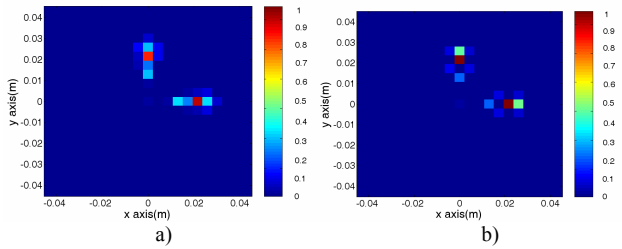

Figure 3. 2D focused data coronal view at: a) z=0 cm, b) z=5cm.

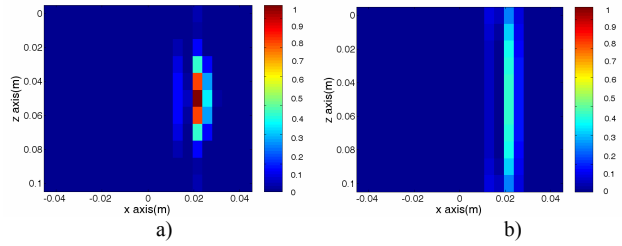

Figure 4. Sagital view at y=0 cm of a) 3D focused data, b) 2D focused data.

V. CONCLUSION

A novel technique for 3D BMI reconstruction was presented in this paper. The proposed method uses the phase differences produced by the different signal travel times in order to determine the spatial location of the target reflections. A series of operations are performed on the spectrum of the collected data in order to migrate it from its original spatial-temporal frequency space to a spatial frequency space. The proposed method presented an average execution time of 4 minutes when 10 planes with 72 scan location per plane were used. The proposed method yielded promising results when applied to simulated data.

ACKNOWLEDGMENTS

This work was funded in part by CancerCare Manitoba and the Natural Sciences and Engineering Research Council of Canada.

REFERENCES

[1] Ahmedin Jemal, Taylor Murray, Elizabeth Ward, Alicia Samuels, Ram C. Tiwari, Asma Ghafoor, Eric J. Feuer and Michael J. Thun, "Cancer Statistics, 2005," CA a Cancer Journal for Clinicians, American Cancer Society, Vol. 55, pp. 10-30, 2005.

[2] Mammography and Beyond: Developing Techniques for the Early Detection of Breast Cancer. Washington, DC: Inst. Med., Nat. Academy Press, 2000.

[3] A. J. Surowiec, S. S. Stuchly, J. R. Barr, and A. Swarup, "Dielectric properties of breast carcinoma and the surrounding tissues," IEEE Transactions on Biomedical Eng., vol. 35, pp. 257–263, Apr. 1988.

[4] Xu Li and S.C Hagness, "A confocal microwave imaging algorithm for breast cancer detection", IEEE Microwave and Wireless Components Letters, vol. 11, pp. 130 – 132, March 2001

[5] D. Li, P. M. Meaney and K. D. Paulsen "Conformal microwave imaging for breast cancer detection," IEEE Transactions on Microwave Theory and Techniques, vol. 51, pp. 1179-1185, Apr. 2003

[6] E. C. Fear and M. A. Stuchly, "Microwave detection of breast cancer," IEEE Transactions on Microwave Theory and Techniques, vol. 48, pp. 1854 – 1863, Nov. 2000.

[7] D. Flores-Tapia, and G. Thomas, "Breast microwave imaging and focusing based on range migration techniques," 16th Int. Zurich Symposium on Electromagnetic Compatibility, Topical Meeting on Biomedical EMC, vol. 1, pp. 75-80, Zurich Switzerland, February 2005.

[8] E.C. Fear, Xu Li, S.C. Hagness, M.A. Stuchly, "Confocal Microwave Imaging for Breast Cancer Detection: Localization of Tumors in Three Dimensions", IEEE Transactions in Biomedical Engineering, vol. 49, pp. 812-821, Aug. 2002

[9] J. Fortuny-Guasch, J.M Lopez-Sanchez, "Extension of the 3-D range migration algorithm to cylindrical and spherical scanning geometries", IEEE Transactions on Antennas and Propagation vol 49, pp. 1434 – 1444, Oct. 2001

[10] M. Soumekh, Synthetic Aperture Radar Signal Processing with MATLAB Algorithms, Wiley-Interscience, New York, 1999.

[11] A. Papoulis, Systems and Transforms with Applications in Optics, McGraw-Hill, New York 1968.